

## MRI measurements of steady state and transient behaviour of fresh cement pastes

Sébastien Jarny<sup>1,2</sup>, Nicolas Roussel<sup>2</sup>, Robert Le Roy<sup>2</sup> and Philippe Coussot<sup>1</sup>

<sup>1</sup> Laboratoire des Matériaux et des Structures du Génie Civil – UMR 113, Institut Navier, Champs sur Marne, France.

<sup>2</sup> Laboratoire Central des Ponts et Chaussées, Division Bétons et Composites Cimentaires, Paris, France.

### ABSTRACT

From MRI measurements we show that in a flowing cement paste thixotropic effects dominate over short time scales while aging effects become significant over larger timescales. The steady state behavior, defined as flow properties in the intermediate period, exhibits a yielding behavior which differs from the prediction of usual yield stress models: the transition from the "solid" to the "liquid" regime is abrupt, so that the shear rate turns suddenly from zero to a finite value (critical shear rate) when the shear stress overcomes a critical value. These critical shear rate and shear stress are independent of the flow conditions and so that they may be considered as intrinsic material parameters. We also show that these results are consistent with usual macroscopic observations from conventional rheometry.

### INTRODUCTION

Cement pastes are colloidal suspensions in which the particle interactions may lead to the formation of various microstructures. Depending on how such structures respond to an applied shear stress or strain rate, one observes different types of macroscopic flow behaviour (Mewis and Spaull<sup>1</sup>, Bird et al.<sup>2</sup>, Coussot and Ancey<sup>3</sup>). The usual ways for describing steady state flow of fresh cement pastes involve Bingham, Herschel-Bulkley, Ellis, Casson or Eyring rheological

models (Atzeni et al.<sup>4</sup>). In practice one determines macroscopic variables such as the torque and the rotation rate with a rotating geometry (Couette, parallel disks) and deduces the parameters of one of the above models. From a systematic comparison of these models in the case of Portland cement pastes Atzeni et al.<sup>4</sup> concluded that the Herschel-Bulkley and Eyring models, which both involve a yield stress, appropriately represent the non-linear shear rate/shear stress curve of cement pastes. Yahia and Khayat<sup>5</sup> also studied the influence of the choice of one of the above models on the fitted yield stress value.

This approach nevertheless neglects the possible strong heterogeneity of the shear rate distribution in non-Newtonian materials within rheometers. Indeed, for example in Couette flows with yield stress fluids, flow occurs only in a region close to the inner cylinder where the local shear stress is larger than a critical value (the yield stress?). The thickness of this region decreases with the applied torque. This strong heterogeneity in the shear rate distribution can significantly affect the apparent behavior of the material since the effective (local) shear rate may widely differ from the apparent shear rate (relative velocity to gap ratio), and should be taken into account for comparison between theory and experiments. In order to avoid this heterogeneity, small gap Couette geometries

are generally used. However, no matter how small the gap is, there will be an unsheared zone in the gap if the applied shear rate is sufficiently low, or when the applied shear stress approaches the yield stress. Moreover it is critical to know whether this shear localization is time-dependent or not, since this effect could be an additional source of time variations of the apparent viscosity (see the observations of Salmon et al.<sup>6</sup> for micellar solutions). The only way to deal with these phenomena consists to carry out measurements of local flow properties and interpret them in rheological terms, an approach which requires specific tools.

Here we present a rheological study of the behavior of cement pastes with the help of a Couette viscometer inserted in a MRI making it possible to measure the local velocity field during transient and steady state flows. Since the local shear stress distribution is well controlled in such a Couette flow we can associate the (measured) local shear rate to the local shear stress and deduce the effective (local) constitutive equation of the material.

## MRI VELOCIMETRY

Among many potentialities, proton Magnetic Resonance Imaging (MRI) provides a powerful means to probe fluids dynamics. This technique is part of nuclear magnetic resonance (NMR) techniques, and uses magnetic properties of hydrogen nuclei (protons) in order to get spatially resolved physico-chemical or dynamic information inside a wide range of samples. These protons are often part of the fluid itself (e.g. water in our samples). Thereafter, no tracers are required to perform measurements.

In the present study, proton NMR velocity measurements were carried out with a Bruker Biospec 24/80 DBX imager located at LMSGC, France. It is equipped with a 0.5T vertical magnet (20MHz proton frequency, diameter: 40 cm), with shielded gradient coils delivering a gradient of 50mT/m, and with a linear birdcage RF coil of 24 cm length and 20 cm inner diameter.

For the purpose of such coupled MRI-rheometry experiments, a home made Couette rheometer was used, specifically designed to comply with MRI constraints. The relatively large scale of samples it can accept makes it suitable for studying civil engineering materials containing coarse particles (cement, concrete, muds, granular pastes, etc.). All the parts of the apparatus inserted in the magnet were built with non-magnetic materials and the motor was moved away as far as possible from the magnet entrance. We used a coaxial cylinder viscometer (inner cylinder:  $r_1 = 40.7$  mm (radius), length:  $h = 113.5$  mm) with a fix outer cylinder (radius  $r_2 = 59.3$  mm) as shown on Fig. 1. The surfaces of the outer and inner cylinder in contact with the fluid were covered with sandpaper with an equivalent roughness of 200  $\mu\text{m}$ . In contrast with most previous works in the MRI field this rheometer is vertical, like usual laboratory rheometers. The rotating axis lies on two bearings situated at its two extremities. The entire system is set up on a pneumatic jack: its lowest position sets the cylinder out of the magnet so that the tools or the samples can easily be removed or set up, while its highest position is such that the shear geometry is at the magnet center. The samples can also be set up during axis rotation so that the time interval between the end of mixing and preshear is short. The imposed rotation velocity  $\Omega$  can be varied over a wide range (from 0.002 to 1000 rpm) by adding a reducer after the direct current (dc) motor. This rheometer is remotely controlled via a computer and the velocity can be imposed step by step or by (almost) continuous ramps. The temperature of the material in the Couette geometry could not be controlled but the room temperature was kept between 20° and 24°.

MRI velocity measurements inside the Couette cell were obtained according to the method first introduced by Hanlon et al.<sup>7</sup> and further modified by Raynaud et al.<sup>8</sup>.

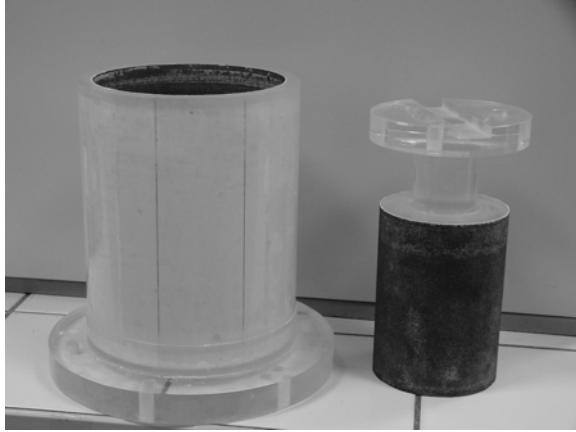


Figure 1. Modified rough inner and outer cylinders of the MRI rheometer.

## MATERIALS AND PROCEDURE

### Mix fitting

We chose to use white cement instead of classical cement in order to minimize C4AF amount in the material. Indeed, Fe paramagnetic oxides enhance relaxation kinetic, thus leading to very poor signal to noise ratio. As the cement particles had to be stable for at least one hour (nor static sedimentation neither dynamic segregation during testing) a viscosity agent was added. After a series of preliminary (rheometrical) tests with different materials we chose the mix fitting given in Table 1 which provided a cement paste with a rheological behavior well representative of the various tested batches, i.e. yield stress and shear thinning behavior, obvious structuration at rest and time dependency as observed by other authors<sup>10</sup>. The W/C value of our cement paste was 0.35.

Component	Mass [g]
White cement CEM I 52.5 Calcia « Cruas »	2000
Superplasticizer optima 100 Chryso	46.7
Nano silica Rhoximat Rhodia	177
Distilled Water	530.3

Table 1. Cement paste composition

### Preparation procedure

The superplasticiser was introduced in the water and the obtained solution was mixed at 260 rpm for 60 s. The white cement and the nanosilica particles were then added. The obtained suspension was mixed at 700 rpm for 15 min and then at 260 rpm for 15 min. This (long) mixing aims at giving the superplasticiser enough time to play its full role in the mixture. The end of preparation corresponds to time  $T_0$ .

### Rheometry

Conventional rheometrical tests were carried out during the first hour following mixing at  $T_0 + 02$  min,  $T_0 + 16$  min,  $T_0 + 29$  min and  $T_0 + 42$  min (Fig. 2), with a HAAKE ViscoTester ® VT550. The inner cylinder and outer cylinder radii  $r_1$  and  $r_2$  were respectively 18.9 mm and 21.0 mm. The inner cylinder height  $h$  was 56.5 mm. Before each measurement, a pre-shear at  $150 \text{ s}^{-1}$  was applied to each sample. Then the apparent shear rate was increased step by step from  $0.5 \text{ s}^{-1}$  to  $120 \text{ s}^{-1}$ . The shear rate was changed to the next level either because the measured torque  $C$  appeared stabilized or because the maximum step duration (30 s) was reached. The set of apparent shear rate  $\dot{\gamma} = \Omega r_1 / (r_2 - r_1)$  and corresponding, apparent shear stress  $\tau = C / 2\pi h r_1^2$  gave us the apparent flow curve of the material (Fig.2). We fitted a Herschel-Bulkley model and a Bingham model to the flow curve obtained at  $T_0 + 02$  min. The corresponding parameters are  $\tau_0 = 14 \text{ Pa}$ ,  $n = 0.93$ ,  $K = 1.5 \text{ SI}$  (Herschel-Bulkley) and  $\tau_0 = 15 \text{ Pa}$  and  $\eta = 1.1 \text{ Pa.s}$  (Bingham).

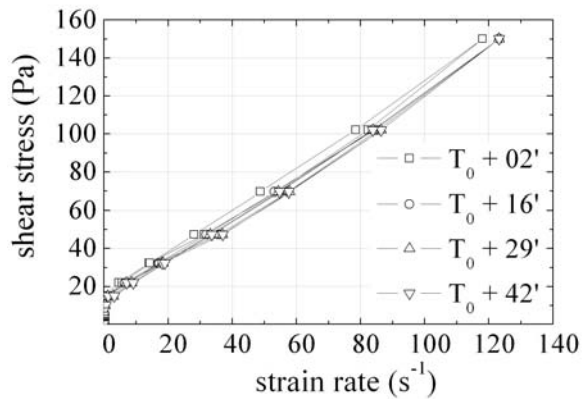


Figure 2. Flow curve of the cement paste at different times after preparation from conventional rheometry.

## MRI RESULTS

### Testing procedure

After a 2 min. preshear at 134 rpm, the rotating speed was immediately switched down to a fixed value between 10.3 and 103.1 rpm at which it was left during half an hour. Throughout the test, the velocity field was determined every 10 seconds. A new sample was prepared before each test under a new rotating speed.

### Steady state experimental results

A typical set of fluid velocity in time at different distances from the axis under a given rotating speed of the inner cylinder is shown in Fig. 3. In a first stage there is a relatively rapid evolution of the velocity: close to the inner cylinder it slightly decreases, far from the inner cylinder the velocity strongly decreases until apparent stoppage at the critical radius beyond which no velocity was recorded from the initial time. Then beyond about 100 s of flow the velocity starts to increase at a stronger rate for larger distances. However these trends concerning the velocity field can naturally be put in qualitative correspondence with the evolutions of viscosity and internal structure of cement pastes in time as described by Otsubo et al.<sup>10</sup> and Banfill<sup>11</sup>. In this context we suggest the following interpretation of our data: over short timescales (our first stage) flocculation and

deflocculation processes dominate, which lead to rapid thixotropic (reversible) effects, while over larger timescales hydration processes dominate, which lead to irreversible evolutions of the local behavior of the fluid. These two effects might in fact act at any time but according to the above scheme they appear to have very different characteristic times. As a consequence it is reasonable to consider that there exists an intermediate period, say around 100s, for which reversible effects have become negligible whereas irreversible effects have not yet become significant. This period corresponds to what we will define as the “steady state” flow regime of the material.

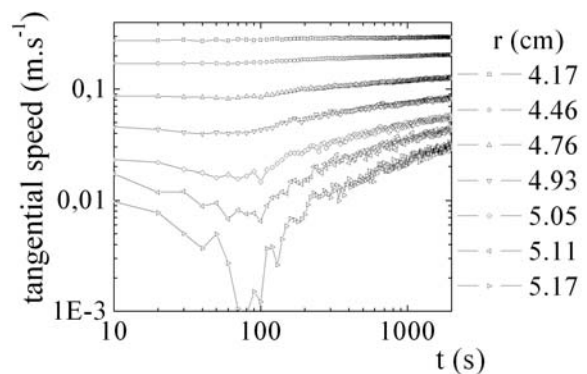


Figure 3. Tangential velocity as a function of time at different radii inside the gap. A point of measure is obtained each 10s. The apparent velocity for distances larger than 5.17 cm was zero within the uncertainty on our measurements. Inner cylinder rotating speed: 82.4 rpm.

The steady state velocity profiles under different rotation velocities ( $\Omega$ ) of the inner cylinder are shown in Figure 4. Note first that, for each level, the velocity extrapolated from these data towards the inner radius almost exactly corresponds to the tangential velocity ( $\Omega r_1$ ) along the rotating cylinder, which indicates that wall slip was negligible. This is not necessarily in contradiction with previous results<sup>12, 13</sup>: indeed here we simply observed that the velocity difference between the material and

the tool is negligible compared to the material velocity in this region, but this difference might become significant under lower rotation velocities, i.e. when the fluid velocity is significantly lower.

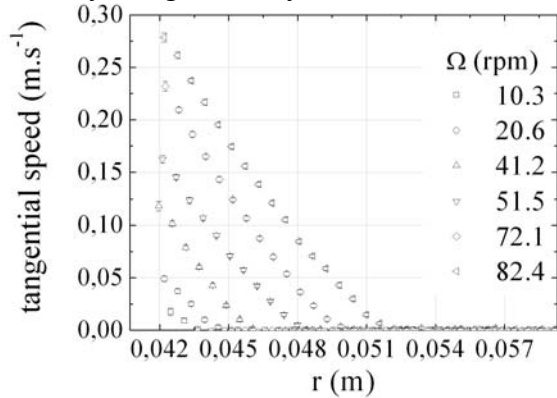


Figure 4. Steady state tangential velocity as a function of radius inside the gap for several inner cylinder rotating speeds after 100 s of flow. Error bars for each measurements are also plotted.

The velocity profiles exhibit two distinct regions: close to the inner cylinder the paste is sheared and the velocity decreases almost linearly as a function of the distance. In the second region the paste apparently does not flow. The interface between these two regions is situated at a critical distance  $r_c$ , which increases with the rotation speed of the inner cylinder: the thickness of the sheared region increases with  $\Omega$ . It is worth noting that the transition between these two regions seems somewhat abrupt in terms of shear rate: the slope of the velocity profile abruptly turns from a finite, constant slope to almost zero, a phenomenon already observed with other thixotropic materials such as bentonite suspensions<sup>14, 15</sup>.

#### Sample homogeneity and water content MRI measurements

Although the abrupt transition spotted in the previous section seems to be intimately linked to the behavior of the homogeneous paste in the case of bentonite suspensions it is not so clear for cement pastes in which the largest solid particles might migrate

through the interstitial liquid during flow. Anyway, it is worth noting that the first velocity profile, measured after 10 seconds of flow, already exhibits distinct sheared and unsheared regions with a slope break at the interface. Since within such a duration a significant migration could hardly have time to develop, this already suggests that, under our experimental conditions, this shear localization basically corresponds to an abrupt behavior transition controlled by stress or strain and not by density change.

The time variations and the steady state aspects of our velocity profiles might partly reflect migration or segregation effects during flow. In particular the farthest regions could be more concentrated in particles and thus have a larger viscosity, which could contribute to the shear localisation. In this context it is necessary to check that the samples remained homogeneous during the tests. In this aim standard relaxation weighted density imaging was carried out. The results, which are not detailed here, permit us to conclude that no heterogeneity in W/C larger than 0.01 developed in the sample during flow.

#### Analysis in terms of a simple yield stress model

As a first approximate yield stress models predict a shear localization as observed here, so that it is natural to expect that a usual (simple) yield stress model can be fitted to our data in steady state. Indeed all these models predict that no flow should occur beyond a critical distance at which the shear stress equals the yield stress. The predictions of the models (here we focus on the Bingham and Herschel-Bulkley models) in terms of velocity within a Couette flow can be determined numerically (analytical solutions only exist for integer values of the power coefficient and in particular for a Bingham model) from the integration of the momentum and constitutive equations. We thus can compare these predictions to our experimental profiles by fitting the parameters. It appears that the measured

velocity profiles are fundamentally different from those expected for fluids following such ideal yield stress models. Indeed, at any scale of observation, these models predict a continuous transition from sheared to unsheared region, i.e. the shear rate, and thus the slope of the velocity profile, continuously tends to zero at the approach of the interface between the sheared and the unsheared regions<sup>16</sup>. In practice this means that it is not possible to find rheological parameters which would relevantly (under three natural criteria, see Fig. 5) fit the measured local velocity.

In particular, with the Bingham model, the values obtained for the plastic viscosity differ from those determined from conventional rheometry (Fig. 2). Moreover, the shapes of the theoretical and experimental velocity profiles significantly differ whatever the rheological parameters. With the Herschel-Bulkley model, the constitutive equation obtained when one tries to have the same unsheared thickness corresponds to shear-thickening ( $n > 1$ ), which is in strong disagreement with the results from conventional rheometry. With the other criteria (Fig. 5) the rheological parameters are in good agreement with those of the usual approach. However, it remains impossible to find a set of  $\tau_0$ ,  $n$  and  $K$  parameters such that the velocity profile fulfils our three basic criteria. To compare the values of the parameters, it is necessary to check that the same range of shear rates is studied in both approaches. The range of apparent shear rates is  $[1 \text{ s}^{-1}; 120 \text{ s}^{-1}]$  for the conventional rheometry results (Fig. 2) and the range of local shear rates is  $[10 \text{ s}^{-1}; 50 \text{ s}^{-1}]$  for the MRI results. These ranges are close enough for the comparison to be licit.

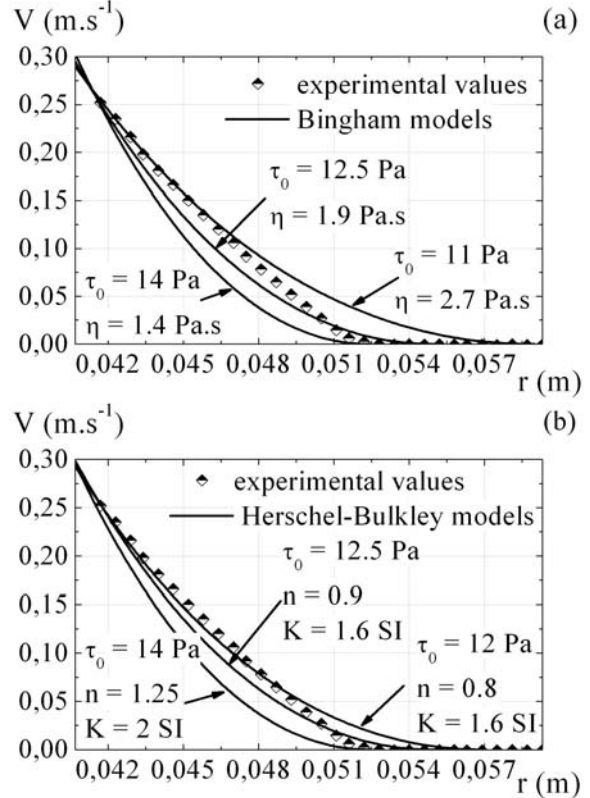


Figure 5. Velocity as a function of distance within the gap of a Couette flow for a 72.1 rpm rotating speed after 100 s. Continuous lines correspond to the predictions using various best fits of the Bingham (a) and Herschel Bulkley model (b) with different conditions: same unsheared thickness, similar slope in the sheared region, same overall shape.

## CONCLUSION

From MRI measurements we have shown that a cement paste exhibits a yielding behavior which differs from the prediction from usual models: the transition from the solid (below  $\tau_c$ ) to the liquid regime (above  $\tau_c$ ) is abrupt, so that the shear rate turns suddenly from zero to a finite value  $\dot{\gamma}_c$  when the shear stress overcomes  $\tau_c$ . Since in addition this cement paste mix fitting had been chosen because its apparent mechanical behavior was representative of that of a large range of cement pastes it is likely that our conclusions apply to most cement pastes.

## REFERENCES

1. Mewis, J. and Spaul, A.J.B. (1976), "Rheology of concentrated dispersions", *Adv. Colloid Interface Sci.*, **6**, 173-200.
2. Bird, R.B., Gance, D. and Yarusso, B.J. (1982), "The rheology and flow of viscoplastic materials", *Rev. Chem. Eng.*, **1**, 1-70.
3. Coussot, P. and Ancey, C. (1999), "Rheophysical classification of concentrated suspensions and granular paste", *Phys. Rev. Lett. E*, **59**, 4445-4457.
4. Atzeni, C., Massidda, L. and Sanna, U. (1985), "Comparison between rheological models for Portland cement pastes", *Cem. Concr. Res.*, **15**, 511-519.
5. Yahia, A. and Khayat, K.H (2001), "Analytical models for estimating yield stress of high performance pseudo-plastic grout", *Cem. Concr. Res.*, **31**, 731-738.
6. Salmon, J.B., Manneville, S. and Colin, A. (2003), "Shear-banding in a lyotropic lamellar phase. Part I: Time-averaged velocity profiles", *Phys. Rev. E*, **68**, 051503.
7. Hanlon, A.D., Gibbs, S.J., Hall, L.D., Haycock, D.E., Frith, W.J. and Ablett, S. (1998), "Rapid MRI and velocimetry of cylindrical Couette flow", *Magn. Reson. Imag.*, **16**, 8, 953-961.
8. Raynaud, J.S, Moucheront, P., Baudez, J.C., Bertrand, F., Guilbaud, J.P. and Coussot, P. (2002), "Direct determination by NMR of the thixotropic and yielding behavior of suspensions", *J. Rheol.*, **46**, 709-732.
9. Shaughnessy, R. and Clark, P.E. (1988), "The rheological behaviour of fresh cement pastes", *Cem. Concr. Res.*, **18**, 327-341.
10. Otsubo, Y., Miyai, S. and Umeya, K. (1980), "Time-dependent flow of cement pastes", *Cem. Concr. Res.*, **10**, 631-638.
11. Banfill, P.F.G. and Saunders, D.C. (1981), "On the viscometric examination of cement pastes", *Cem. Concr. Res.*, **11**, 363-370.
12. Saak, A.W., Jennings, H.M and Shah, S.P. (2001), "The influence of wall slip on yield stress and viscoelastic measurements of cement pastes", *Cem. Concr. Res.*, **31**, 205-212.
13. Nehdi, M. and Rahman, M.-A. (2004), "Estimating rheological properties of cement pastes using various rheological models for different test geometry, gap and surface friction", *Cem. Concr. Res.*, Accepted for publication, Uncorrected proof available online.
14. Coussot, P., Nguyen, Q.D., Huynh, H.T. and Bonn, D. (2002), "Viscosity bifurcation in thixotropic, yielding fluids", *J. Rheol.*, **46**, 3, 573-589.
15. Roussel, N., Le Roy, R. and Coussot, P. (2004), "Test of a thixotropy model by comparison with local and macroscopic flow properties", *J. Non-Newtonian Fluid Mech.*, **117**, 85-95.
16. Jarny, S. and Coussot, P. (2002), "Characterization of paste flows in a Couette geometry", *Rhéologie*, **2**, 52-63, (in French).